IEEE Access
Multidisciplinary | Rapid Review | Open Access Journal

Received 22 June 2023, accepted 24 July 2023, date of publication 1 August 2023, date of current version 16 August 2023.

Digital Object Identifier 10.1109/ACCESS.2023.3300588

RESEARCH ARTICLE

Hopfield Neural Network Based Uplink/Downlink Transmission Order Optimization for Dynamic Indoor TDD Femtocells

MIRZA NAZRUL ALAM[1], RIKU JÄNTTI[2], (Senior Member, IEEE), AND ZEKERIYA UYKAN[3], (Senior Member, IEEE)

[1]Wirepas Oy, 33720 Tampere, Finland
[2]School of Electrical Engineering, Department of Communications and Networking, Aalto University, 02150 Espoo, Finland
[3]College of Engineering and Technology, American University of the Middle East, Egaila 54200, Kuwait

Corresponding author: Zekeriya Uykan (zekeriya.uykan@aum.edu.kw)

ABSTRACT The Uplink/Downlink transmission mode or Transmission Order (TO) optimization has recently appeared as a new optimization domain in radio resource management. Such optimization is a combinatorics problem and requires good heuristic algorithm to be approximately solved within short time for the dynamic radio environment. This paper shows how the TO optimization problem in Time Division Duplex (TDD) indoor femtocells can be formulated and solved by the Hopfield Neural Network (HNN) based TO schedulers. Both centralized and distributed versions are analyzed in the context of indoor femtocells. We also examine proposed TO schedulers' system performance in TDD indoor femtocells environment by extensive simulation campaigns. Our simulation results for a large 3-story building including 120 femtocells show that (i) the indoor femtocell system performance is improved up to 13 to 20 percent by the proposed HNN schedulers depending on the number of femtocells, (ii) the proposed TO schedulers converge within the first few epochs. (iii) The performance of the proposed schedulers are justified by a time-consuming but a thorough Genetic Algorithm Scheduler.

INDEX TERMS Dynamic-TDD, femtocell networks, hopfield neural network, transmission order optimization, genetic algorithm.

I. INTRODUCTION AND MOTIVATION

In recent years, small cell deployment is a top priority for many operators and tens of millions of small cells have been deployed worldwide, most of which are indoor [1]. Various reports forecast that the global small cell networks market is expected to grow at a CAGR (compound annual growth rate) of about 9% during the period 2022-2030 and the *indoor* small cell networks segment is the highest contributor to the market (see e.g. [1]). Consequently, the vast majority of the wireless traffic originates from or terminates at an indoor environment. Therefore, to address the demand for the exponentially increasing wireless data traffic in the years to come, we need intelligent Radio Resource Management (RRM) tools especially for in-building wireless systems. RRM includes various mechanisms like power control, channel allocation, scheduling, handover, etc [51], [59], [60]. To meet the ever-increasing wireless data demand, we should get the most out of the RRM mechanisms. Recently, a new RRM mechanism for TDD systems, called uplink/downlink Transmission Order (TO) is introduced which can run on top of all other RRM mechanisms independently, and the authors in [7] in 2016 show that the uplink/downlink TO has a great potential to remarkably outperform the traditional case where both uplinks and downlinks are separately synchronized. However, we argue that the benefits of the TO (transmit order) optimization in the RRM has been "somehow overlooked" in literature since the work in [7] in 2016 and thus the potential system performance gains of the TO optimization have not been explored in literature.

The associate editor coordinating the review of this manuscript and approving it for publication was Olutayo O. Oyerinde.

Therefore, our motivation in this paper is to ''remind'' the importance of the TO optimization. In this paper, we focus on the indoor femtocell environment due to its increasing importance and show that the system performance is remarkably improved (i.e., up to 13 to 20 percent depending on the number of femtocells) at the expense of some extra signaling and calculations by the proposed HNN-based TO schedulers.

To address the sharp rise of the network densification, the 3GPP introduced enhanced X2 interface and mobility features in Release 12 [26] for scalability and seamless handover in the small cell networks. Other enhancement includes Machine to Machine (M2M) communications, self-organizing networks (SON), proximity services etc. Small Cell Network has emerged as one of the key solutions for enhancing network capacity because it greatly decreases the minimum frequency reuse distance. The 3GPP report [31] also suggests that future small cell networks operate with or without the coverage of macro network and support both ideal and non-ideal backhaul [32].

Currently, the most common form of small cells are femtocells. The deployment of femtocells has gained the attention of the academia and the industry for its ability to improve the indoor coverage and offload the major portion of traffic of macro base stations. In our study, it is assumed that the femtocell network is assigned an orthogonal frequency band in the overlaid macro network or it operates as an isolated network because of the following reasons: (a) The cross-tier interference in an overlaid network could be mitigated by optimizing various RRM mechanisms such as sub-channel assignment, power allocation techniques, etc [21], [22], [28], [57] and (b) the metal coated structure of the modern energy efficient building wall introduces additional 20-30 dB penetration loss over the old building for the radio signal [29], [30].

For improving the system performance of femtocell networks, most of the prior works mainly addressed the traditional RRM mechanisms like spectrum assignment [19], [53] power control [20], [25], [50], [58], clustering and resource allocation [21], [56] interference and mobility management [54], joint power control and spectrum assignment [22], multiple antenna deployment to exploit the angle dimension [23], [24], etc. In [23], the femto base station inserts null in the direction of UE (User Equipment) that belongs to the microcell during the transmission. The power control technique mainly increases the user experience of the macro UEs in the proximity of the femtocell network by reducing the outage probability. Besides all these radio resource management (RRM) mechanisms, recently a novel optimization dimension, called Transmission Order (TO), has been introduced, which could possibly be implemented on top of all above-mentioned RRM mechanisms in Time Division Duplexing (TDD) femtocell networks. To the best of our knowledge, this is the first paper addressing the TO optimization in indoor femtocell networks (small cell networks).

In TDD systems, the uplink and downlink transmissions are multiplexed in time using the same carrier frequency. It is noted in [2] that in case of Heterogeneous Networks all cells do not have to have the same UL–DL timing. In TDD based femtocell system, the interference between cells can sometimes be reduced and the capacity can be improved by setting an offset between the frame timings such that uplinks of some frames coincide with downlinks of another frame [3]. The prospects and challenges of UL/DL configuration in LTE TDD are studied in [26] and [27] and it is concluded that UL/DL reconfiguration will play a vital role in future wireless mobile communications.

In dynamic TDD [4], the transmission direction in a slot is assigned dynamically. Therefore, in a particular slot, the direction of transmission of all the femtocells may not be in the same direction. Therefore, for N femtocells, the number of combination or set of transmission mode for any slot is 2^N, which yields an NP (Nondeterministic Polynomial time)-complete problem for relatively large N.

The authors in [5] and [6] formulate a joint UL/DL TO and channel allocation problem and propose some centralized and distributed algorithms for the D2D communications underlying TDD cellular systems. It's shown in [6] that TO optimization algorithms can remarkably improve the performance of D2D communications. In [7], a graph representation is proposed for the TO optimization problem to examine the performance of the D2D communications underlying cellular TDD networks. TO optimization is applied to Heterogeneous Networks in [33].

In this paper, we extend the works in [5], [6], and [7] to formulate the TO optimization problem in the framework of the Hopfield Neural Network (HNN) [8], [9] and propose the HNN-based uplink/downlink TO schedulers for the indoor TDD femtocells. HNNs [8], [9] have been one of the most well-known and widely used neural networks for optimization since 1980s. Hopfield and Tank presented the application of HNN in optimization problems in [9] by solving the classical Travelling-Salesman Problem (TSP). This application of HNNs made it a very popular model in optimization in early 80s, and since then HNN has been applied to many different areas from associative memory systems design problems to radio resource optimization in wireless networks, combinatorial optimization to image restoration, etc. among many others. For further details and description of the HNN, see e.g., [49]. Our main motivation and reason of exploring and proposing the ''HNN based TO schedulers'' is threefold:

(i) A recent paper of Uykan [45] shows the link between the HNN and the pioneering interference reduction algorithm GADIA [36]. Using statistical physics theory, Babadi and Tarokh thoroughly proved the optimality of the GADIA under some statistical conditions in [36]. On the other hand, the paper [45] shows that the HNN turns out to be a special case of the GADIA. This implies that HNN-based solutions would be expected to yield sufficiently good results for the standard indoor COST 231 channel model [37] investigated in this paper as well.

(*ii*) The HNN based solutions are fast enough for solving the TO optimization in indoor TDD femtocells. To be precise, the VLSI implementation of the HNN has the capacity to find solutions in a few microseconds [10], which is much less than the coherence time of typical indoor channels. As an outdoor channel example, typical channel coherence times for WiMAX at the mobile speed of 2 km/h are about 200 ms and 93 ms at 2.5 GHz and at 5.3 GHz, respectively [48]. Even at the mobile speed of 45 km/h, the channel coherence time for WiMAX at 2.5 GHz is 10 ms [48].

(*iii*) Recently, deep learning based solutions and neural networks based methods for solving various wireless communications problems have become a hot research topic trend thanks to the improving computational resources on devices and the availability of data in large quantity [46], [47]. Our paper is also in line with this research trend presenting a neural network-based solution to the TO optimization problem for indoor TDD femto-cells.

The HNN has successfully been applied to various real-time RRM optimization problems like solving dynamic channel allocation problem [10], [11], [12], multiuser detection [13], [14], phase noise mitigation [15], peak to average power reduction in orthogonal frequency division duplex (OFDM) system [16], among many others. The contributions of this paper can be summarized as follows:

A. CONTRIBUTIONS OF THIS PAPER

In this paper:

(a) We continue the work in [7] by extending it to the TDD indoor femtocells. Here, we convert the TO optimization problem of TDD indoor femtocells into the HNN optimization formulation.

(b) To the best of our knowledge, the performance improvement of the indoor femtocell networks by the TO optimization has not been studied yet, and so this is the first paper addressing the TO optimization in indoor femtocell networks. In this paper, we analyse TDD indoor femtocell networks data rate improvements by the proposed HNN based TO algorithms running extensive simulation campaigns. The simulation results for a large 3-story building including 120 femtocells show that the indoor femtocell system performance is improved up to 13 to 20 percent by the proposed HNN schedulers as compared to the standard TO cases.

(c) The justification of the simulation results in this paper is twofold: (i) The GADIA-HNN equivalence recently shown in [45]. (ii) All the simulation results of the proposed HNN-based algorithms for the indoor simulation scenarios (using the standard COST 231 channel model) in Section V are justified by comparing them with those of a time-consuming but thorough Genetic Algorithm (GA) [17], [18] scheduler, which acts as an approximation of the global solution.

(d) The proposed HNN based TO schedulers that minimize the total network interference can run on top of any other RRM mechanisms mentioned above. Thus, our scheme is independent of any RRM mechanisms.

The rest of the paper is organized as follows: Section II presents the formulation of the problem. The proposed HNN based schedulers for the TO optimization problem are presented and analysed in Section III. Section IV explains the experimental setup, presents computer simulations results and a discussion part. The conclusions are given in Section V, followed by Appendices.

II. FORMULATION

Let's consider a system of N femtocells each of which has a Femto Access Point (FAP) and a mobile station (MS) using the same channel. Then all FAP-MS pairs interfere each other as shown in Fig. 1. In this system, FAPs are numbered by *(0,1,2,3,….,N-1)* and the MSs are numbered by *(N, N+1,N+2,……,2N-1)*. For the sake of simplicity, in our notation, the MS (i+N) is served by the FAP i. This yields that $g_{ii} = g_{i,i+N}$ for UL (from MS (i+N) *to FAP (i))* or $g_{ii} = g_{i+N,i}$ for DL (from FAP (*i*) *to MS (i+p))*. This implies that the node i and node (i+N) are receiver-transmitter pairs as shown in Fig. 1, where *i=0,1,2,..N-1*. For each pair, the UL or DL order is determined by its TO. If TO is UL (i.e., +1), then transmitter is MS (i+N), and receiver is FAP i. Otherwise, if TO is DL (i.e., -1), then transmitter is FAP i, and receiver is MS i+N. So, there are $2N$ nodes represented by the set $V = \{0,1,2,..,2N-1\}$.

The received signal power g_{ij} can be modeled as follows [34]:

$$g_{ij} = \frac{s_{ij}c_{ij}}{d_{ij}^{\beta}} p_j, \quad i,j = 1, 2, \ldots, N \tag{1}$$

where p_j is the transmit power of transmitter j; s_{ij} is the shadow fading term, d_{ij}^{β} is propagation loss in a link with pathloss exponent β, and c_{ij} is multipath fading factor [34], [35]. As in many other studies, we, in this paper, assume flat fading and slow fading channel case, and the channel coherence time is much higher than the radio resource management algorithms runtime, which is true especially for the indoor wireless environments where the mobility is naturally low.

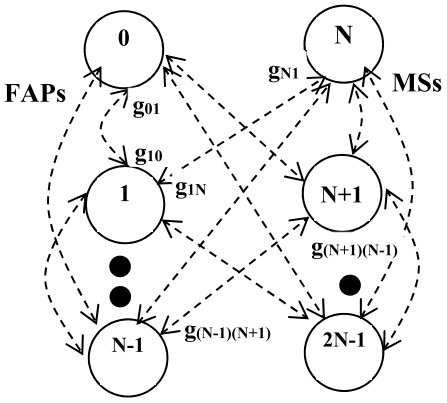

FIGURE 1. A femto network of N cells showing the potential interfering received signal powers. The MS $i+N$ is served by the FAP i.

Let S_R and S_T represent the sets of indices of N receivers and N transmitters, respectively, depending on the TOs. So, the received Signal-to-Interference+Noise-Ratio (SINR) at receiver i is calculated by [34]

$$\gamma_i = \frac{g_{i,own}}{\sigma_i^2 + \sum_{j \in S_T} g_{ij}}, \quad i \in S_R, j \in S_T \tag{2}$$

where, γ_i is the received SINR at receiver i, σ_i^2 is the thermal noise at receiver i and g_{ij} is the received signal power at receiver i for the signal sent from transmitter j, and $g_{i,own}$ represents the own (desired) signal received power.

As explained in Section I (page 3), in TDD based femtocell system, the interference between cells can sometimes be reduced and the capacity can be improved by setting an offset between the frame timings such that uplinks of some frames coincide with downlinks of another frame [3], [26], [27]. This yields two UL/DL configurations for our femtocell network, which we call "TO-mode 1" and "TO-mode 2": In "TO-mode 1", those FAPs and MSs in set S_T are transmitters and the rest (i.e., those FAPs and MSs in set S_R) are receivers. On the other hand, "TO-mode 2" is opposite of "TO mode 1". In other words, the transmission directions are reversed in "TO-mode 2" so that those FAPs and MSs in set S_R become transmitters and those FAPs and MSs in set S_T are receivers.

Determining the TOs represented by the sets S_R and S_T, the sum of the total network interference in TO-mode 1 is

$$I^{ntw}_{mode\_1}(S_T, S_R) = \sum_{i \in S_R} \sum_{j \in S_T} g_{i,j} \tag{3}$$

Similarly, sum of the total network interference in TO-mode 2 is

$$I^{ntw}_{mode\_2}(S_T, S_R) = \Sigma_{i \in S_R} \Sigma_{j \in S_T} g_{i,j} \tag{4}$$

From (3) and (4), the total network interference, denoted as I^{ntw}_{tot}, is

$$I^{ntw}_{tot}(S_T, S_R) = I^{ntw}_{mode\_1} + I^{ntw}_{mode\_2} \tag{5}$$

The TO optimization problem is formulated as determining the optimum sets S_T and S_R which minimize the total network interference in eq.(5), i.e.,

$$min(S_T, S_R)\, I^{ntw}_{tot}(S_T, S_R) \tag{6}$$

For the sake of convenience, our notation is summarized in TABLE 1.

TABLE 1. Notation table.

$g_{i,j}$	The received signal power at receiver i for the signal sent from transmitter j.
S_T and S_R	sets of indices of N transmitters (FAPs and MSs) and N receivers (FAPs and MSs), respectively, depending on their TOs.
I^{ntw}_{tot}	total network interference which is minimized during the TO optimization process.
$I^{ntw}_{mode\_1}(t)$	total network interference in TO mode-1
$I^{ntw}_{mode\_2}(t)$	total network interference in TO mode-2
W	Augmented *2N-by-2N* matrix of the received-signal powers. **W** also corresponds to the weight matrix of the HNNSv1.
x	the TO vector of the augmented HNNv1 system **W** in such a way that $x_n = -x_{n+N}$, *n=0,1,2,..N-1* +1:UL and -1:DL
Ω	*N-by-N* matrix of the received-signal powers. Ω also corresponds to the weight matrix of the HNNSv2.
y	the TO vector of the HNNv2 system **W.** +1:UL and -1:DL

III. HOPFIELD NEURAL NETWORK BASED TO SCHEDULER

As illustrated in Fig.1, the system of N femtocells now can be modeled with a directed interference graph *G(V,E)* where the vertices V are the nodes and the edges E represent interference powers [7], [52]. The edge g_{ij} denotes the interference power at node i caused by transmitter j, where *i,j∈{0,1,..., 2N-1}*. A transmit node is not assumed to interfere with itself $g_{ii} = 0$ nor does it interfere with the intended receiver $g_{i,(i+N)} = 0$. The division of transmitters into two time slots corresponds to partitioning of the interference graph in Fig.1 ([7]). In the same time slot, some cell may transmit in DL direction while others transmit in UL direction. In the next time slot, the cells change their transmission direction.

Definition: A schedule $\boldsymbol{x}$=(x_n, *n=0,1,...,2N-1*), $x_n \in \{-1, +1\}$ *defines a graph partitioning such that* (S_T, S_R) *divides the set of vertices V into two sets* $S_T = \{n : x_n = 1\}$ *and* $S_R = \{n : x_n = -1\}$ *such that*

1. *All nodes are scheduled* $V = S_T \bigcup S_R$
2. *Number of transmitters and receivers are the same:* $|S_T| = |S_R| = N$
3. *For a TO, a node is either transmitter or receiver: In other words, if* $n \in S_T$ *then* $(n + N) \notin S_T$, $x_n = -x_{n+N}$, *n=0,1,2,..N-1.*

Clearly a schedule corresponds to partitioning of the interference graph in Fig. 1, but not all partitions correspond to a schedule. For example, in Fig. 1, a feasible schedule vector $\boldsymbol{x}$ = *{-1 1 -1 1 -1 1}* corresponds to the set S_T = *{1, 3, 5}* and S_R= *{0, 2, 4}*. However, for example, the partition S_T = *{1, 4, 5}* and S_R = *{0, 2, 3}* does not correspond to a schedule.

Lemma 1: Let's define a discrete-value vector **x** *such that* $x_i \in \{-1, +1\}$ and $x_i = -x_{i+N}$, for *i=0,1,2,..N-1. The total network interference power in eq.(5) due to schedule* **x** *is*

$$I^{ntw}_{tot}(S_T, S_R) = \frac{1}{4} \sum_{ij} g_{ij}(x_i - x_j)^2 = \frac{1}{4} x_T(D - G)x \tag{7}$$

where **D**=diag(d_n, *n=0,1,...,2N-1*) is a diagonal matrix containing the row sums of **G**, i.e., $d_i = \sum_{j=0}^{2N-1} g_{ij}$.

Proof: Following the steps in [6] for our system of $2N$ nodes, we straightforwardly get the eq.(7).

Lemma 2: The system link interference matrix $\boldsymbol{G}$ *above is an asymmetric 2Nx2N dimensional matrix. The total interference power in (1) due to schedule* $\mathbf{x}$ *can be turned into the following symmetric case*

$$\begin{aligned} min\, I_{tot}^{ntw}(S_T, S_R) &= min\, I_{tot}^{ntw}(\boldsymbol{x}) = min\, \boldsymbol{x}^T \boldsymbol{W} \boldsymbol{x} \\ \mathrm{x}_n &= -x_{n+N}, \quad n = 0, \cdots, N-1 \end{aligned} \tag{8}$$

where $\boldsymbol{W}$=-$\boldsymbol{G}$-$\boldsymbol{G}^T$ *is symmetric matrix and* $\boldsymbol{x} \in -1, 1\}^{2N}$.

Proof: The proof of this Lemma is given in Appendix A.

Proposition 1: The TO optimization problem in eq.(6) can be turned into the well-known HNN optimization framework, which means the TO optimization problem in (6) can be solved by the traditional (N-by-N dimensional) HNN.

Proof: Because in a $2N$-dimensional schedule $x_n = -x_{n+N}$, n=0,1,2,..,N-1, we define a new N-dimensional vector $\mathbf{y}$ such that $\mathbf{x}^T = [\mathbf{y}^T, -\mathbf{y}^T]$. So, $\mathbf{x} \in \{-1, 1\}^{2N}$ and $\boldsymbol{y} \in \{-1, 1\}^N$. From Lemma 2 and eq.(7), we obtain

$$\begin{aligned} &I_{tot}^{ntw}(S_T, S_R) = I_{tot}^{ntw}(\boldsymbol{y}) \\ &= \frac{1}{4}\boldsymbol{y}^T (\boldsymbol{D_1} + \boldsymbol{D_2} - \boldsymbol{G_{11}} + \boldsymbol{G_{12}} + \boldsymbol{G_{21}} - \boldsymbol{G_{22}})\boldsymbol{y} \\ &= -\frac{1}{8}\boldsymbol{y}^T (\boldsymbol{D_1} + \boldsymbol{D_2} + \boldsymbol{G_{11}} + \boldsymbol{G_{11}^T} + \boldsymbol{G_{22}} \\ &\quad + \boldsymbol{G_{22}^T} - \boldsymbol{G_{12}} - \boldsymbol{G_{12}^T} - \boldsymbol{G_{21}} - \boldsymbol{G_{21}^T})\boldsymbol{y} \end{aligned} \tag{9}$$

where

$$\boldsymbol{G} = \begin{bmatrix} \boldsymbol{G_{11}} & \boldsymbol{G_{12}} \\ \boldsymbol{G_{21}} & \boldsymbol{G_{22}} \end{bmatrix} \quad \text{and } \boldsymbol{D} = \begin{bmatrix} \boldsymbol{D_1} & 0 \\ 0 & \boldsymbol{D_2} \end{bmatrix} \tag{10}$$

Note that $\boldsymbol{y}^T(\boldsymbol{D_1} + \boldsymbol{D_2})\boldsymbol{y} = \sum_{n=0}^{2N-1} d_n = constant$, for any $\boldsymbol{y} \in \{-1, 1\}^N$, and thus has no effect on the minimization. It is worth to mention that volume of matrix G ($vol(G)$) is constant during the coherence time of the channel due to the flat fading assumption. Hence, defining vector $\boldsymbol{y} \in \{-1, 1\}^N$, the TO optimization problem in eq.(6) can be written as

$$min\, I_{tot}^{ntw}(S_T, S_R) = min\, I_{tot}^{ntw}(\boldsymbol{y}) = min\, \boldsymbol{y}^T \boldsymbol{\Omega} \boldsymbol{y} \tag{11}$$

where

$$\begin{aligned} \boldsymbol{\Omega} = \boldsymbol{G_{11}} + \boldsymbol{G_{11}^T} + \boldsymbol{G_{22}} + \boldsymbol{G_{22}^T} - \boldsymbol{G_{12}} \\ - \boldsymbol{G_{12}^T} - \boldsymbol{G_{21}} - \boldsymbol{G_{21}^T} \end{aligned} \tag{12}$$

As seen from eq.(11), the right-hand side is equivalent to minimizing the energy (Lyapunov) function of the HNN whose weight matrix is $\boldsymbol{\Omega}$, which completes the proof.

A. CENTRALIZED HNN BASED TO SCHEDULER V.1 (HNNSV1)

The matrix $\mathbf{W}$ in eq.(8) is a symmetric matrix because $w_{ij} = 0.5\left(g_{ij} + g_{ji}\right)$. From (8), we can run a $(2N \times 2N)$-dimensional HNN with the constraint $x_n = -x_{n+N}$, n=0,1,2,..N-1 as follows:

$$\begin{aligned} \boldsymbol{x_i(t+1)} &= \boldsymbol{sign}\left\{\sum_{j=0}^{2N-1} \boldsymbol{w_{ij} x_j(t)}\right\} \\ \text{s.t.} \quad \boldsymbol{x_n} &= -\boldsymbol{x_{n+N}} \text{ and } \quad \boldsymbol{n = 0, 1, \cdots, N-1} \end{aligned} \tag{13}$$

where $i = 0, 1, \cdots, 2N-1$. This scheduler, called HNNSv1, is summarized in TABLE 4 in Appendix C. Each state in the HNN consists of either -1 or +1 as discussed in section II. Basically, the RRC (Radio Resource Control) layer co-ordinates the measurements and associated reporting task. The RRC command determines what to measure, how to measure, over which frequency the measurements will take place, when to send feedback report etc. As far as the central unit in HNNSv1 is concerned, the Femto Access Points (FAPs) or HeNBs (Home eNB) could communicate with the common server or central unit through the Gateway (GW). The central unit will keep coordination among the femtocells. Every now and then, all the devices will measure the pilot or Reference Signal Received Power (RSRP) of the other transmitters in the networks. These measured data will be destined at the common server or the central FAP unit. It is noteworthy that LTE-A supports X2 interface between two FAPs or HeNBs regardless of the presence of HeNB-GW. The introduction of the new interface facilitates the FAPs to exchange information between them directly and within real time.

B. CENTRALIZED HNN BASED TO SCHEDULER V.2 (HNNSV2)

In the HNNSv1 above, the dimension of the weight matrix W was $2N \times 2N$. From Proposition 1 and eq.(11), we can run $(N \times N)$-dimensional HNN without any constraints for the weight matrix $\boldsymbol{\Omega}$ as follows:

$$y_i(t+1) = sign\left\{\sum_{j=0}^{N-1} \Omega_{ij} y_j(t)\right\}, i = 0, 1, \cdots, N-1 \tag{14}$$

where matrix $\boldsymbol{\Omega_{ij}}$ is the ij'th entry of matrix $\boldsymbol{\Omega}$ defined by eq.(12). This scheduler is called HNNSv2 and is summarized in **TABLE 5** in Appendix C.

C. HNN BASED DISTRIBUTED TO SCHEDULER (HNNDS)

Examining eq.(13), we see that the term $\sum_{j=0}^{2N-1} w_{ij} x_j(t)$ is in fact the total co-channel interference power received by the node i in the femtocell network. So, the TO optimization could be performed in a fully distributed fashion because each FAP-MS pair can regularly measure the interference powers from the other nodes. Our distributed scheduler is called HNNDS and is presented in TABLE 6 in Appendix C.

In this distributed approach, all the FAPs and MSs in the network sequentially measure the interferences and update their schedule one at a time. From eqs.(3), (4) and (12), we obtain

$$\boldsymbol{x_i(t+1)} = \boldsymbol{sign}\left\{\boldsymbol{I_{slot_1}^{ntw}(t) - I_{slot_2}^{ntw}(t)}\right\} \tag{15}$$

TABLE 2. A comparison of the proposed TO schedulers.

HNNSv1	$x_i(t+1) = sign\left\{\sum_{j=0}^{2N-1} w_{ij}x_j(t)\right\}$ where $i = 0, 1, \cdots, 2N-1$, and under the constraint $x_n = -x_{n+N}$, n=0,1,..., N-1, from (13)
HNNSv2	$y_i(t+1) = sign\left\{\sum_{j=0}^{N-1} \Omega_{ij}y_j(t)\right\}$ where $i = 0, 1, \cdots, N-1$, from (14)
HNNSDS	$x_i(t+1) = sign\{I^{ntw}_{slot\_1}(t) - I^{ntw}_{slot\_2}(t)\}$ where $i = 0, 1, \cdots, N-1$ from (15)

The proposed centralized and distributed TO schedulers are summarized in TABLE 2.

Comparing eqs.(13) and (14) with the state update of a neuron in the standard discrete Hopfield Neural Network (e.g. see eq.(3.27) in the textbook [49], p.3-13), we conclude that they both are the same, which shows that our proposed model in this paper can be solved by the standard discrete HNN.

IV. SIMULATION RESULTS

A. EXPERIMENTAL SETUP

An extensive simulation study is performed to evaluate and justify the efficiency of the proposed TO schedulers. In our simulations we use the indoor environment of a three-story large office building [37] shown in Fig.2, and the standard COST 231 indoor propagation model of [37]. For all the assumptions, see Section V of [37] where the pathloss is defined in B.1.8. This model is the extension of the Hata model where the carrier frequency is 1.5 GHz to 2 GHz. Each floor of the office building consists of forty rooms [44].

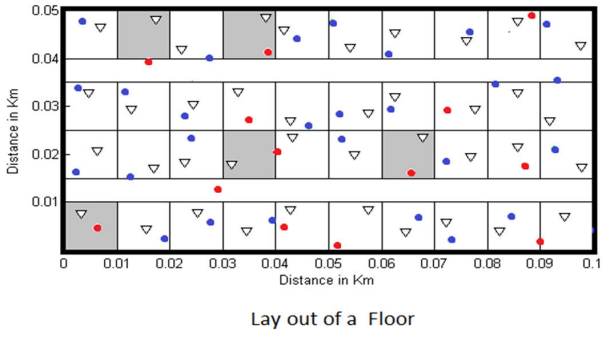

FIGURE 2. Layout of a floor in a three-story office building.

In Fig.2, FAPs and MSs are marked as triangles and small circles, respectively. The red MS means the corresponding FAP↔ MS link is in active state, i.e., either it is in downlink or in uplink transmission. The shaded room implies that the link is in downlink transmission in a particular time slot. In the deployed scenario, FAPs are randomly deployed in each room of the office building. Each FAP serves only one MS. The network performance is measured by gradually increasing the activation probability of the link. The traffic in all direction is full buffered. The transmission power of FAP and MS are assumed to be the same while measuring the performance of HNNSv1 and HNNSv2 and is set to 23 dBmW. For distributed algorithm HNNDS, the performance is examined for unequal transmission power of 20 dBmW and 23 dBmW for FAP and MS respectively. The results of the simulation for different activation probability of links are averaged over 100 independent snapshots (realizations).

B. NUMERICAL ANALYSIS

In this subsection, the performances of the proposed TO schedulers are examined. In sub-section *B.1*, the convergence speed in terms of the number of epochs is investigated. In subsection *B.2*, the performance of the centralized HNNSv1 and HNNSv2 in terms of network interference, link SINR as well as additional link capacity is examined in details. In the last subsection *B.3*, the performance of the HNNSDS is examined and compared with the centralized HNNSv1. There are two reference algorithms: (1) All UL and DL are separately synchronized without any TO optimization (standard case) and (2) the TOs are randomly chosen.

1) B1) COMPARISON OF CONVERGENCE SPEEDS IN TERMS OF EPOCHS

In our simulations, three-story building and forty rooms on each floor yields 120 femtocells. So, for 10% active links corresponds to 12 active femtocells on the average. Fig. 5 depicts the average and maximum number of epochs that the proposed centralized TO schedulers HNNSv1 and HNNV2 take to converge as number of active links increases. Here, an epoch is defined as one batch during which all links are sequentially updated once.

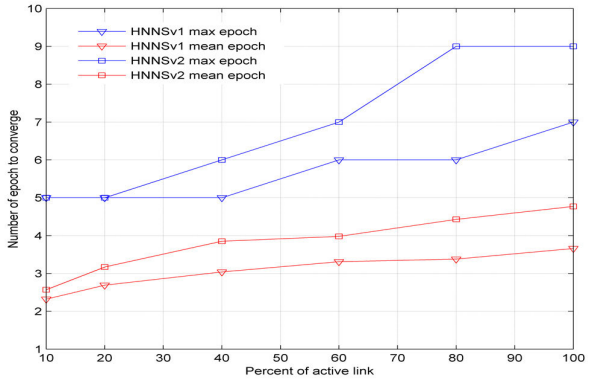

FIGURE 3. Maximum and Average number of epochs with respect to the active link ratio (100% ratio corresponds to 120 femtocells).

Fig.3 shows that both centralized schedulers, HNNSv1 and HNNv2, take few to several epochs to converge depending on the number of active links in the network. As seen from the figure, massive increase of search space does not influence the convergence speed in terms of the epoch number.

On the other hand, as far as the convergence time is concerned, it is expected that the HNNv2 be much faster

than the HNNSv1 is because (i) the number of variables in HNNSv1 is twice the number of variables in HNNv2, and (ii) unlike the HNN2, the HNNSv1 has some extra calculations to check and meet the constraint for each update. In order to examine the convergence speeds, the codes have been written in C++ and the program has been compiled in C++14 and the high-resolution clock functions are used to measure the execution time. The results are averaged over 1000 random snapshots and show that the HNNSv2 is almost thousand times faster than the HNNSv1 is.

2) B2) THE SYSTEM PERFORMANCE OF CENTRALIZED HNNSv1 AND HNNSv2

The 5^{th} and 95^{th} percentile as well as the median of the average total network interference and average link SINR are presented in Fig. 4 and Fig. 5, respectively, as the active link ratio increases. For example, 100% and 50% active links correspond to 120 and 60 femtocells, respectively. Both Fig.4 and Fig.5 confirm the superior performance of the proposed TO schedulers as compared to the reference case. For example, the improvement is in between 3 dB to 6 dB for the 60% active link case. Furthermore, Fig.4 and Fig.5 also show that the performance of the HNNSv1 and HNNSv2 is very close to the GASch, which represents a benchmark of the global optimum approximately.

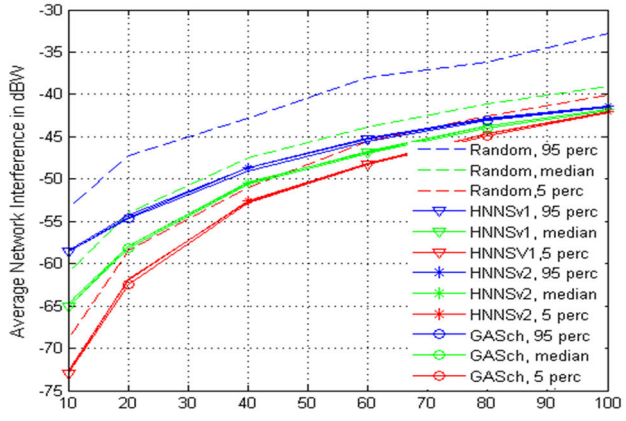

FIGURE 4. Percentiles of the total network interference with respect to the active link ratio for various TO schedulers.

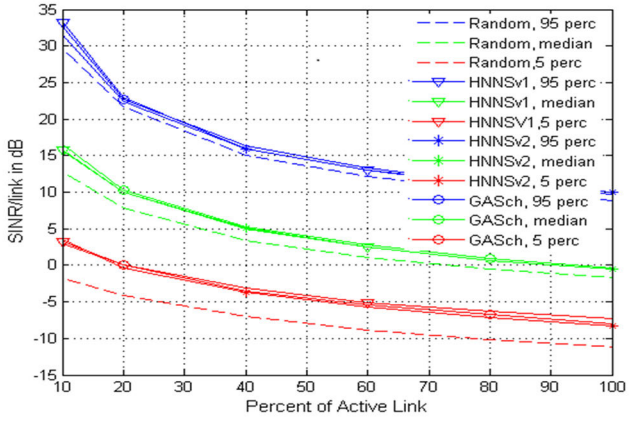

FIGURE 5. Percentiles of link SINR with respect to the active link ratio for various TO schedulers.

Given the SINR, corresponding capacity is calculated by the Shannon's formula for each case. The percentage of the corresponding additional link capacity, denoted by C_{add}, is defined as

$$C_{add} = \left(C_{opt} - C_{rnd}\right) \times 100/C_{rnd} \tag{16}$$

where C_{opt} represents the link capacity obtained by a TO optimization (e.g. HNNSv1) and C_{rnd} shows the link capacity obtained by determining the TOs randomly without optimization. The percentage of additional link capacity is plotted in Fig. 6.

Fig.6 shows that HNSv1 and HNNSv2 offer additional 15 to 20 percent capacity gain as compared to the reference case and the gain depends on the number of active femtocells. The GASch gives slightly better additional gain than the HNSv1 and HNNSv2 do, but the detailed GASch used in our simulations is too slow to apply in the wireless environment. The role of the thorough GASch is to justify the results of the proposed HNNSv1, HNNv2 and HNNDS as mentioned above. For the details of the GA, see Appendix B.

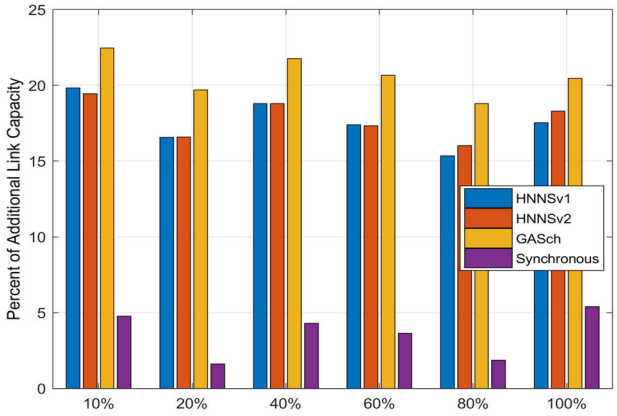

FIGURE 6. Percent of additional link capacities for different active link ratios.

3) B3) THE CONVERGENCE SPEED AND SYSTEM PERFORMANCE OF HNNDS

Fig.7 shows that the HNNDS (distributed scheduler) converges within few epochs regardless of the number of active links in the network as the centralized scheduler HNNSV1 does. The average number of epochs in the HNNDS case is slightly higher than that of the HNNSv1 case. This is because the HNNSv1 has constraints to meet, unlike the HNNDS (see TABLE 2). The results in Fig.7 are in line with those of Fig.3.

The additional link capacity gains of the HNNDS (distributed) and HNNSv1 (centralized) are shown in Fig.8. The reference case is the same as before. Fig.8 shows that

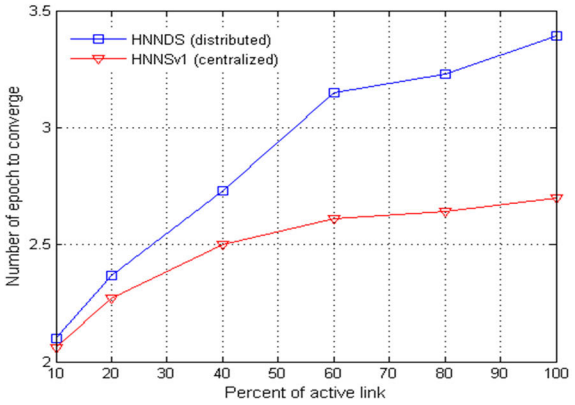

FIGURE 7. Average number of epochs with respect to the active link ratio (100% ratio corresponds to 120 femtocells).

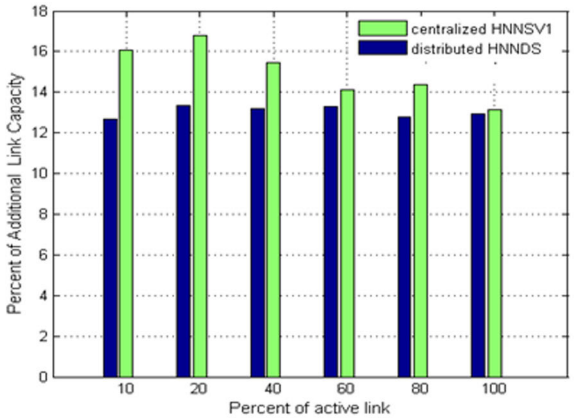

FIGURE 8. Comparison of centralized (HNNv1) and distributed (HNNDS) versions for different active link ratios.

the additional capacity provided by the HNNDS is around 13 percent and is about 1 to 3 percent less than the centralized scheduler HNNSv1 depending on the number of femtocells (active link ratio) in our 3-story building scenario.

C. DISCUSSION

Although our TO optimization formulation given by eq.(3)-(6) is originally for the symmetrical UL and DL load conditions, it is also valid for the asymmetrical load conditions. This is because for the TDD systems, UL and DL transmission is done in the same frequency band, and therefore UL and DL capacity can be adjusted based on demand. In theory this is an advantage over the Frequency Division Duplex (FDD) systems. In a typical FDD system where UL transmissions use a seperate frequency band which is just as large as the DL frequency band (e.g. 5 MHz for UMTS), then those FDD systems have a 1:1 ratio between UL and DL. On the other hand, with the TDD systems, this ratio can be changed, for example to 2:1, 3:1, etc. in order to give more capacity to DL. For example, it is reported in [38], [39], and [40] that 3:2 DL to UL ratio is suitable to address almost all common wireless traffic loads. In this case, one set of transmitters (the FAPs and MSs in set S_T) transmit in a DL-DL-UL-UL-DL frame and the rest of the transmitters (the FAPs and MSs in set S_R) can transmit the frame UL-UL-DL-DL-DL during the optimized TO mode. The last slot here is dedicated for DL and therefore first four slots are kept flexible for the TO optimization purposes. As compared to the TO-mode 1 (TO1) and TO-mode 2 (TO2) defined on p3, we see that, for a given transmitter, DL-DL-UL-UL-DL corresponds to TO1-TO1-TO2-TO2-TO1, and UL-UL-DL-DL-DL corresponds to TO2-TO2-TO1-TO1-TO1. Fig.6 shows that around 15 percent additional capacity gain can be achieved per slot by the proposed TO schedulers for the 3-story building, and thus the 3:2 frame yields about $(4 \times 15\%)/5{=}12\%$ additional link capacity per frame by the HNNSv1, HNNSv2 and HNNDS as compared the reference case (uplink and downlink are separately synchronized). So, without any HARQ ambiguity [41] or complexity, the proposed TO schedulers could be transferable to the 3GPP LTE TDD and METIS projects [61], [62] which pave the ways of 5G standards.

V. CONCLUSION

In this paper, we extend the work in [7] to the TDD indoor femtocell case, and our investigations yield various novel results, some of which are as follows:

(*i*) We formulate the TO optimization problem in TDD indoor femtocells in the framework of the HNN optimization.

(ii) We design two centralized and one distributed TO schedulers, all of which are based on the HNN.

(iii) An extensive indoor simulation study of a 3-story large building consisting of 120 femtocells is performed to examine the performance of the proposed TO schedulers. The standard COST 231 channel model is used. The results show that the indoor system data rate is improved up to 13 to 20 percent as compared to the standard TO cases for our 3-story building. The results of the proposed TO schedulers have also been justified by a time-consuming but thorough Genetic Algorithm based TO scheduler that acts as a benchmark of global solution approximately.

TABLE 3. Summary of GA steps.

1. Initialize some random population. The number of populations is equal to the size of the mating pool declared. Set generation, *GEN=0*.
2. Fill the mating pool with selected individuals. Do Selection based on fitness value.
3. Perform Crossover operation on the selected individuals in the mating pool with crossover probability P_c.
4. Perform Mutation operation on the selected individuals in the mating pool with mutation probability P_m.
5. Increase *GEN*.
6. If *GEN* reaches the desired generation number, take the best solution found so far. Otherwise repeat the steps from 2.

TABLE 4. HNN-based to scheduler v1 (HNNSv1).

1.	Over several time slots, every MS and its serving FAP measure the corresponding interferences from each node of the femto network, and send the interference powers to a central unit (e.g. central FAP).
2.	The central FAP sets the weight matrix of the HNN as $\mathbf{W} = -\mathbf{G}\text{-}\mathbf{G}^{\mathrm{T}}$. The dimension of $\mathbf{W}$ is $2N$ by $2N$.
3.	The HNN (sequentially) runs according to (13) in the central unit with the constraint $x_i = - x_{i+N}$. The new pair elements are allowed to change *only if* the total interference power is further reduced.
4.	Steps 1 to 3 are repeated sequentially until the total network interference converges to a stable state (i.e., until any of the TOs does not change any more).

(iv) The proposed HNN based TO schedulers that minimize the total network interference can run on top of all other RRM mechanisms. Thus, our scheme is independent of any other RRM mechanisms.

This work can be extended to different directions: For example, in our paper, our simulator is semi-dynamic, which means that the results are averaged over random channel realizations (snapshots) as done in many other papers. Developing a fully dynamic simulator where the indoor mobility of the MSs is explicitly modelled and analysing the effect of the full mobility on the TO mechanism would be an interesting future research direction. The effect of the beamforming on the TO system performance would be another interesting future research subject.

APPENDIX A

Proof of Lemma 2: From Lemma 1 (eq. (7)), the total UL network interference is

$$I_{\text{tot}}^{\text{ntw}}(S_T, S_R) = I_{\text{tot}}^{\text{ntw}}(\boldsymbol{x}) = \frac{1}{4}\boldsymbol{x}^T\boldsymbol{D}\boldsymbol{x} - \frac{1}{4}\boldsymbol{x}^T\boldsymbol{G}\boldsymbol{x} \tag{17}$$

The diagonal elements in equation (17) have no impact on the optimization of the quadratic form as the first part $\boldsymbol{x}^T\boldsymbol{D}\boldsymbol{x} = \sum_n d_n$ is constant. The *Hermitian splitting* of the matrix is $\mathbf{G}$ is given by $\boldsymbol{G} = \frac{1}{2}\left(\boldsymbol{G} + \boldsymbol{G}^T\right) + \frac{1}{2}\left(\boldsymbol{G} - \boldsymbol{G}^T\right)$ where the first part is symmetric, and the latter part is skew symmetric. For any $\boldsymbol{x} \in \{-1, 1\}^{2N}$, $\frac{1}{2}\boldsymbol{x}^T\left(\boldsymbol{G} - \boldsymbol{G}^T\right)\boldsymbol{x} = \mathbf{0}$. Hence, minimization of $I_{\text{tot}}^{\text{ntw}}(\boldsymbol{x})$ in eq.(7) can be written as eq.(8), which completes the proof.

APPENDIX B

GENETIC ALGORITHM BASED TO SCHEDULER (GASCH)

The GA is a stochastic algorithm whose search method models some natural phenomena, i.e., the genetic inheritance and the Darwinian strife for survival [17], [18], [43]. Basically, GA searches in the entire search space to find the global optimum [55]. After sufficient number of generations together with suitable parameters, its outcomes become close to the global optimum. Therefore, in this paper we use a slow but thorough GA scheduler for justification of the performance of our proposed TO schedulers (HNNSv1, HNNv2 and HNNDS) in our simulations.

The GA undergoes some basic core operations e.g., Selection, Crossover and Mutation. Before describing the core operators, some basic terms are defined below:

OBJECTIVE FUNCTION

It is the function whose value needs to be optimized. In our case, it is the total network interference in eq.(5).

CHROMOSOME

Chromosome is any arbitrary solution represented as a string of bits. In this paper, a chromosome is defined by vector $\boldsymbol{y} \in \{-1, 1\}^N$

OFFSPRINGS

Offsprings are the new chromosomes or solution after the crossover operation takes place between two chromosomes.

FITNESS FUNCTION

An evaluation function that rates the individual solution according to their fitness value. In this paper, the smaller the interference is the higher fitness value is.

Some core operators [42], [43] in our slow but thorough GASch are described below:

SELECTION

Based on the fitness value, the selection process selects a finite number of solutions or chromosome for the mating pool from a randomized set of solutions. How many copies of a particular chromosome will be transferred to the new mating pool depends on its fitness value. There exists a number of selection operators. In our GASch, the most common roulette-wheel selection process is used.

CROSSOVER

Selection process only picks up good solutions but does not create new probable solutions. Crossover operator does this. Crossover exchanges some property between two randomly selected chromosomes.

There are variants of crossover. In our algorithm, two-point crossovers are used where two cross sites are selected randomly along the string length.

TABLE 5. HNN-based to scheduler v2 (HNNSv2).

1. Every MS and its serving FAP measure the interferences from each node of the network, and send them to a central unit (e.g., central FAP).
2. The central FAP sets the weight matrix of the HNN, $\mathbf{\Omega}$, as in (12). The dimension of $\mathbf{\Omega}$ is N by N.
3. The HNN (sequentially) runs according to (14) without any constraints and updates the elements x_i of vector $\mathbf{x}$.
4. Steps 1 to 3 are repeated sequentially until the total network interference converges to a stable state (i.e., until any of the TOs does not change any more).

TABLE 6. HNN Distributed Scheduler (HNNDS).

1. Every FAP-MS pair $i, (i + N)$ in a network stops its transmission for a while to measure the network interferences. Every MS and its serving FAP measure the corresponding interferences from corresponding pilot signals in the two slots separately.
2. Based on the measurements, every FAP-MS pair update its TO schedule according to equation (15) sequentially.
3. Steps 1 to 2 are repeated sequentially by each FAP-UE pair in a fully distributed fashion until the total network interference converges to a stable state (i.e., until any of the TOs does not change any more).

MUTATION

The mutation operation mimics the mutation phenomenon occurs at some stage on chromosome in natural evolution process. In this operation bits of the chromosome of mating pools are altered with mutation probability P_m. The typical range of P_m is 0.001 to 0.5. In our GASch, the P_m is taken as 0.001. Mutation guarantees the diversity among individuals and explores new individuals in the search space.

The major steps of the GA summarized in TABLE 3 are used in our detailed GASch.

APPENDIX C

See Tables 4–6.

REFERENCES

[1] (Dec. 6, 2022). *Small Cell Networks Market, Straight Research*. Accessed: Dec. 22, 2022. [Online]. Available: https://straitsresearch.com/report/small-cell-networks-market

[2] W. Wang, G. Yu, and A. Huang, "Cognitive radio enhanced interference coordination for femtocell networks," *IEEE Commun. Mag.*, vol. 51, no. 6, pp. 37–43, Jun. 2013.

[3] S. Bin Ali, C.-H. Yu, O. Tirkkonen, and C. Ribeiro, "Optimization of dynamic frame offset in time division duplex system," in *Proc. IEEE 73rd Veh. Technol. Conf. (VTC Spring)*, May 2011, pp. 1–5.

[4] W. Jeong and M. Kavehrad, "Cochannel interference reduction in dynamic-TDD fixed wireless applications, using time slot allocation algorithms," *IEEE Trans. Commun.*, vol. 50, no. 10, pp. 1627–1636, Oct. 2002.

[5] Z. Uykan and R. Jäntti, "Joint optimization of transmission-order selection and channel allocation for bidirectional wireless links—Part I: Game theoretic analysis," *IEEE Trans. Wireless Commun.*, vol. 13, no. 7, pp. 4003–4013, Jul. 2014.

[6] Z. Uykan and R. Jäntti, "Joint optimization of transmission-order selection and channel allocation for bidirectional wireless links—Part II: Algorithms," *IEEE Trans. Wireless Commun.*, vol. 13, no. 7, pp. 3991–4002, Jul. 2014.

[7] Z. Uykan and R. Jäntti, "Transmission-order optimization for bidirectional device-to-device (D2D) communications underlaying cellular TDD networks—A graph theoretic approach," *IEEE J. Sel. Areas Commun.*, vol. 34, no. 1, pp. 1–14, Jan. 2016.

[8] J. J. Hopfield, "Neural networks and physical systems with emergent collective computational abilities," *Proc. Nat. Acad. Sci. USA*, vol. 79, no. 8, pp. 2554–2558, 1982.

[9] J. J. Hopfield and D. W. Tank, "'Neural' computation of decisions in optimization problems," *Biol. Cybern.*, vol. 55, pp. 141–146, Jul. 1985.

[10] C. W. Ahn and R. S. Ramakrishna, "QoS provisioning dynamic connection-admission control for multimedia wireless networks using a Hopfield neural network," *IEEE Trans. Veh. Technol.*, vol. 53, no. 1, pp. 106–117, Jan. 2004.

[11] Z. Uykan, "Fast-convergent double-sigmoid Hopfield neural network as applied to optimization problems," *IEEE Trans. Neural Netw. Learn. Syst.*, vol. 24, no. 6, pp. 990–996, Jun. 2013.

[12] O. Lazaro and D. Girma, "A Hopfield neural-network-based dynamic channel allocation with handoff channel reservation control," *IEEE Trans. Veh. Technol.*, vol. 49, no. 5, pp. 1578–1587, Sep. 2000.

[13] G. I. Kechriotis and E. S. Manolakos, "Hopfield neural network implementation of the optimal CDMA multiuser detector," *IEEE Trans. Neural Netw.*, vol. 7, no. 1, pp. 131–141, Jan. 1996.

[14] Z.-W. Zheng, Y.-S. He, F. Zhang, and J. Pan, "HNN-based multiuser detection for uplink CDMA communication system under multipath fading channels," in *Proc. 5th IEEE Int. Conf. Cogn. Informat.*, Jul. 2006, pp. 810–814.

[15] Q. Quan, "A multilevel Hopfield neural network for OFDM system with phase noise," in *Proc. 7th Int. Conf. Inf., Commun. Signal Process. (ICICS)*, Macau, China, Dec. 2009, pp. 1–5.

[16] H. Wang, "PAPR reduction for OFDM system with a class of HNN," in *Proc. Int. Symp. Commun. Inf. Technol.*, Bangkok, Thailand, Oct. 2006, pp. 492–497.

[17] J. H. Holland, *Adaptation in Natural and Artificial Systems*. Ann Arbor, MI, USA: Univ. of Michigan Press, 1975.

[18] J. R. Koza, *Genetic Programming: On the Programming of Computers by Means of Natural Selections*. Cambridge, MA, USA: MIT Press, 1992.

[19] D. Marabissi, D. Tarchi, R. Fantacci, and A. Biagioni, "Adaptive subcarrier allocation algorithms in wireless OFDMA systems," in *Proc. IEEE Int. Conf. Commun. (ICC)*, May 2008, pp. 3475–3479.

[20] V. Chandrasekhar, J. G. Andrews, T. Muharemovic, Z. Shen, and A. Gatherer, "Power control in two-tier femtocell networks," *IEEE Trans. Wireless Commun.*, vol. 8, no. 8, pp. 4316–4328, Aug. 2009.

[21] A. Abdelnasser, E. Hossain, and D. I. Kim, "Clustering and resource allocation for dense femtocells in a two-tier cellular OFDMA network," *IEEE Trans. Wireless Commun.*, vol. 13, no. 3, pp. 1628–1641, Mar. 2014.

[22] A. Barbieri, A. Damnjanovic, T. Ji, J. Montojo, Y. Wei, D. Malladi, O. Song, and G. Horn, "LTE femtocells: System design and performance analysis," *IEEE J. Sel. Areas Commun.*, vol. 30, no. 3, pp. 586–594, Apr. 2012.

[23] G. Bartoli, R. Fantacci, D. Marabissi, and M. Pucci, "LTE-A femto-cell interference mitigation with MuSiC DOA estimation and null steering in an actual indoor environment," in *Proc. IEEE Int. Conf. Commun. (ICC)*, Jun. 2013, pp. 2707–2711.

[24] M. Husso, J. Hamalainen, R. Jantti, and A. M. Wyglinski, "Adaptive antennas and dynamic spectrum management for femtocellular networks: A case study," in *Proc. 3rd IEEE Symp. New Frontiers Dyn. Spectr. Access Netw.*, Chicago, IL, USA, Oct. 2008, pp. 1–5.

[25] A. M. Voicu, L. Simic, and M. Petrova, "Interference mitigation in two-tier LTE networks: Does power control pay off for femtocells?" in *Proc. IEEE 25th Annu. Int. Symp. Pers., Indoor, Mobile Radio Commun. (PIMRC)*, Washington, DC, USA, Sep. 2014, pp. 1332–1337.

[26] *LTE-Evolved Universal Terrestrial Radio Access Network (E-UTRAN); X2 Application Protocol (X2AP)*, 3GPP TS 36.423, Version 12.3.0, Release 12, 2014.

[27] Z. Shen, A. Khoryaev, E. Eriksson, and X. Pan, "Dynamic uplink-downlink configuration and interference management in TD-LTE," *IEEE Commun. Mag.*, vol. 50, no. 11, pp. 51–59, Nov. 2012.

[28] Y. Wu, D. Zhang, H. Jiang, and Y. Wu, "A novel spectrum arrangement scheme for femto cell deployment in LTE macro cells," in *Proc. IEEE 20th Int. Symp. Pers., Indoor Mobile Radio Commun.*, Sep. 2009, pp. 6–11.

[29] I. Rodriguez, H. C. Nguyen, N. T. K. Jorgensen, T. B. Sorensen, and P. Mogensen, "Radio propagation into modern buildings: Attenuation measurements in the range from 800 MHz to 18 GHz," in *Proc. IEEE 80th Veh. Technol. Conf. (VTC-Fall)*, Vancouver, BC, Canada, Sep. 2014, pp. 1–5.

[30] A. Asp, Y. Sydorov, M. Valkama, and J. Niemelä, "Radio signal propagation and attenuation measurements for modern residential buildings," in *Proc. IEEE Globecom Workshops*, Anaheim, CA, USA, Dec. 2012, pp. 580–584.

[31] *Scenarios and Requirements for Small Cells Enhancements for E-URTA and E-UTRAN*, document 3GPP TR 36.932, Version 12.0.0, Dec. 2012.

[32] T. Nakamura, S. Nagata, A. Benjebbour, Y. Kishiyama, T. Hai, S. Xiaodong, Y. Ning, and L. Nan, "Trends in small cell enhancements in LTE advanced," *IEEE Commun. Mag.*, vol. 51, no. 2, pp. 98–105, Feb. 2013.

[33] Z. Uykan and R. Jäntti, "Converged heterogeneous networks with transmit order and base-station-to-base-station interference cancellation," in *Proc. Int. Wireless Commun. Mobile Comput. Conf. (IWCMC)*, Dubrovnik, Croatia, Aug. 2015, pp. 469–473.

[34] T. S. Rappaport, *Wireless Communications: Principles & Practice*, 2nd ed. Upper Saddle River, NJ, USA: Prentice-Hall, 2002.

[35] A. J. Viterbi, *CDMA: Principles of Spread Spectrum Communication*. Reading, MA, USA: Addison-Wesley, 1995.

[36] B. Babadi and V. Tarokh, "GADIA: A greedy asynchronous distributed interference avoidance algorithm," *IEEE Trans. Inf. Theory*, vol. 56, no. 12, pp. 6228–6252, Dec. 2010.

[37] *Selection Procedure for the Choice of Radio Transmission Technology of the UMTS*, document TR 101 112, UMTS 30.03, Version 3.1.0, European Telecommunications Standard Institute (ETSI), 1997.

[38] *5G Slice Load Analysis*. Accessed: Jan. 19, 2023. [Online]. Available: https://www.sandvine.com/

[39] TD-LTE Frame Configuration Primer NSN. *5G Slice Load Analysis*. Accessed: Apr. 2, 2023. [Online]. Available: http://networks.nokia.com/system/files/document/nsn_td_lte_frame_configuration_wp.pdf

[40] *Evolved Universal Terrestrial Radio Access (EUTRA); Physical Channels and Modulations*, document 3GPP TS 36.211, 2016.

[41] C. Wang, X. Hou, A. Harada, S. Yasukawa, and H. Jiang, "HARQ signalling design for dynamic TDD system," in *Proc. IEEE 80th Veh. Technol. Conf. (VTC-Fall)*, Sep. 2014, pp. 1–5.

[42] Z. Michalewicz, *Genetic Algorithms + Data Structures = Evolution Programs*, 3rd ed. Germany: Springer, 1996.

[43] D. E. Goldberg, *Genetic Algorithms in Search, Optimization, and Machine Learning*. Reading, MA, USA: Addison-Wesley, 1989.

[44] M. N. Alam, "Traffic-adaptive and energy-efficient small cell networks energy, delay and throughput," Ph.D. dissertation, Dept. Commun. Netw., Aalto Univ., Espoo, Finland, 2017.

[45] Z. Uykan, "On the working principle of the Hopfield neural networks and its equivalence to the GADIA in optimization," *IEEE Trans. Neural Netw. Learn. Syst.*, vol. 31, no. 9, pp. 3294–3304, Sep. 2020.

[46] H. Ye, G. Y. Li, and B.-H. Juang, "Power of deep learning for channel estimation and signal detection in OFDM systems," *IEEE Wireless Commun. Lett.*, vol. 7, no. 1, pp. 114–117, Feb. 2018.

[47] X. Wang, L. Gao, S. Mao, and S. Pandey, "CSI-based fingerprinting for indoor localization: A deep learning approach," *IEEE Trans. Veh. Technol.*, vol. 66, no. 1, pp. 763–776, Jan. 2017.

[48] J. G. Andrews, A. Ghosh, and R. Muhamed, *Fundamentals of WiMAX: Understanding Broadband Wireless Networking*. Upper Saddle River, NJ, USA: Prentice-Hall, 2007.

[49] M. T. Hagan, H. B. Demuth, and M. Beale, *Neural Network Design*, 2nd ed. New York, NY, USA: PWS Publishing Company, 1996.

[50] S. Suryani, M. Susanto, A. Sadnowo, S. N. Hasim, and F. Hamdani, "Interference management using power allocation for downlink transmission of femtocell-macrocell ultra dense networks," in *Proc. 9th Int. Conf. Inf. Technol., Comput., Electr. Eng. (ICITACEE)*, Aug. 2022, pp. 184–188.

[51] B. Agarwal, M. A. Togou, M. Marco, and G.-M. Muntean, "A comprehensive survey on radio resource management in 5G HetNets: Current solutions, future trends and open issues," *IEEE Commun. Surveys Tuts.*, vol. 24, no. 4, pp. 2495–2534, 4th Quart., 2022, doi: 10.1109/COMST.2022.3207967.

[52] B. Agarwal, M. A. Togou, M. Ruffini, and G.-M. Muntean, "A fairness-driven resource allocation scheme based on a weighted interference graph in HetNets," in *Proc. IEEE Int. Symp. Broadband Multimedia Syst. Broadcast. (BMSB)*, Aug. 2021, pp. 1–6, doi: 10.1109/BMSB53066.2021.9547096.

[53] Z. Li and C. Li, "Femto-cell research on network bilateral spectrum allocation algorithm," in *Proc. IEEE 2nd Int. Conf. Electron. Technol., Commun. Inf. (ICETCI)*, May 2022, pp. 149–157, doi: 10.1109/ICETCI55101.2022.9832227.

[54] M. M. S. Maswood, U. K. Dey, S. Akter, M. A. Uddin, M. M. I. Mamun, S. S. Sonia, and A. G. Alharbi, "Improving system performance in indoor environment by designing femtocell considering interference and mobility management," in *Proc. IEEE 11th Annu. Comput. Commun. Workshop Conf. (CCWC)*, Jan. 2021, pp. 1204–1209, doi: 10.1109/CCWC51732.2021.9376073.

[55] G. Sahu and S. S. Pawar, "Resource allocation using genetic algorithm in heterogeneous network," in *Proc. IEEE Pune Sect. Int. Conf. (PuneCon)*, Dec. 2019, pp. 1–7, doi: 10.1109/PuneCon46936.2019.9105736.

[56] N. Sharma and K. Kumar, "Energy efficient clustering and resource allocation strategy for ultra-dense networks: A machine learning framework," *IEEE Trans. Netw. Service Manage.*, vol. 20, no. 2, pp. 1884–1897, Jun. 2023, doi: 10.1109/TNSM.2022.3218819.

[57] S. Mishra and C. S. R. Murthy, "Increasing energy efficiency via transmit power spreading in dense femto cell networks," *IEEE Syst. J.*, vol. 12, no. 1, pp. 971–980, Mar. 2018, doi: 10.1109/JSYST.2016.2573845.

[58] J. Sultan, W. A. Jabbar, N. S. Al-Thobhani, A. Al-Hetar, and M. Saif, "Interference mitigation using uplink power control in 5G relay-based heterogeneous networks," in *Proc. 2nd Int. Conf. Emerg. Smart Technol. Appl. (eSmarTA)*, Oct. 2022, pp. 1–7, doi: 10.1109/eSmarTA56775.2022.9935380.

[59] Y. Xu, G. Gui, H. Gacanin, and F. Adachi, "A survey on resource allocation for 5G heterogeneous networks: Current research, future trends, and challenges," *IEEE Commun. Surveys Tuts.*, vol. 23, no. 2, pp. 668–695, 2nd Quart., 2021.

[60] M. U. A. Siddiqui, F. Qamar, F. Ahmed, Q. N. Nguyen, and R. Hassan, "Interference management in 5G and beyond network: Requirements, challenges and future directions," *IEEE Access*, vol. 9, pp. 68932–68965, 2021, doi: 10.1109/ACCESS.2021.3073543.

[61] H. Droste, G. Zimmermann, M. Stamatelatos, N. Lindqvist, O. Bulakci, J. Eichinger, V. Venkatasubramanian, U. Dotsch, and H. Tullberg, "The METIS 5G architecture: A summary of METIS work on 5G architectures," in *Proc. IEEE 81st Veh. Technol. Conf. (VTC Spring)*, May 2015, pp. 1–5, doi: 10.1109/VTCSpring.2015.7146131.

[62] Accessed: Jan. 15, 2023. [Online]. Available: https://metis-ii.5g-ppp.eu/index.html

MIRZA NAZRUL ALAM received the B.Sc. degree in electrical and electronic engineering and the M.Sc. degree in telecommunication engineering, and the D.Sc. degree in wireless communications engineering from Aalto University, Finland, in 2017. He is currently a Senior Researcher with Wirepas, Finland. His research interest includes radio resource management, optimization, M2M and D2D communications, energy efficiency, 5G, and application of AI in wireless communications.

RIKU JÄNTTI (Senior Member, IEEE) received the M.Sc. degree (Hons.) in electrical engineering and the D.Sc. degree (Hons.) in automation and systems technology from the Helsinki University of Technology (TKK), in 1997 and 2001, respectively. He is currently a Full Professor in communications engineering and the Head of the Department of Communications and Networking, School of Electrical Engineering, Aalto University, Finland. Prior to joining Aalto, in August 2006, he was a Professor (pro tem) with the Department of Computer Science, University of Vaasa. He is a member of the editorial board of the IEEE TRANSACTIONS ON COGNITIVE COMMUNICATIONS AND NETWORKING. He has also been IEEE VTS Distinguished Lecturer (Class 2016). His research interests include machine type communications, disaggregated radio access networks, backscatter communications, quantum communications, and radio frequency inference.

ZEKERIYA UYKAN (Senior Member, IEEE) received the B.S. and M.S. degrees (Hons.) in electrical engineering from Istanbul Technical University (ITU), Istanbul, Turkey, in 1993 and 1996, respectively, and the Lic.Tech. (Hons.) and Dr.Tech. degrees in electrical engineering from the Helsinki University of Technology (HUT), (now Aalto University), Espoo, Finland, in 1998 and 2001, respectively. He is currently a Full Professor in electrical engineering with the American University of the Middle East, Egaila, Kuwait. He was with Stanford University, CA, USA, from January 2002 to December 2002; a Visiting Scientist with Harvard University, Cambridge, MA, USA, from September 2008 to June 2009; and a Visiting Associate Professor with the COMNET Department, School of Electrical Engineering, Aalto University, from August 2012 to September 2012 and from February 2013 to August 2013. He was with Dogus University, Istanbul, from September 2009 to September 2015, and he has been with the American University of the Middle East, since September 2014. His research interests include the statistical mechanics of learning, artificial intelligence, and wireless communications systems.